The Photochemistry of Riboflavin Tetraacetate and Nucleosides. A Study Using Density Functional Theory, Laser Flash Photolysis, Fluorescence, UV−Vis, and Time Resolved Infrared Spectroscopy

Christopher B. Martin, Xiaofeng Shi, Meng-Lin Tsao, Dale Karweik, James Brooke, Christopher M. Hadad,* and Matthew S. Platz*

Department of Chemistry, The Ohio State University, 100 West 18th Avenue, Columbus, Ohio 43210

Received: May 1, 2002; In Final Form: July 5, 2002

The photoreaction between riboflavin tetraacetate and nucleosides was investigated using time-resolved infrared spectroscopy (TRIR), laser flash photolysis with UV−vis detection, fluorescence quenching, absorption spectroscopy, and density functional theory calculations. Riboflavin tetraacetate (RBTA) was studied experimentally with indole and with Sheu and Foote's organic soluble silylated guanosine (G′). Lumiflavin and (*R*)-2-amino-(*S*)-4-hydroxy-(*R*)-5-(hydroxymethyl)-tetrahydrofuran were used as computational models for RBTA and for the sugar moiety of the nucleoside, respectively, using density functional theory calculations (B3LYP/6-31G* and B3LYP/6-31+G**). Vibrational spectra were also calculated for the transient species. Time-resolved infrared spectroscopic data obtained using RBTA are in excellent agreement with the calculated spectra for the triplet flavin, and in the presence of silylated guanosine, with the formation of the most stable hydroflavin radical, RBTH, by an electron transfer−proton transfer mechanism. Although the gas-phase calculations indicate that abstraction of a hydrogen atom from the sugar is slightly exothermic, this reaction does not proceed at a rate measurable as monitored by TRIR spectroscopy. Singlet RBTA is also quenched by G′ in methylene chloride. Stern−Volmer analysis of the fluorescence quenching data indicates that this reaction proceeds with a rate constant of 8.7×10^8 M^{-1} s^{-1}.

I. Introduction

Riboflavin (vitamin B_2) is found in milk, beer, yeast, and leafy vegetables. It is an important part of a healthy diet. Riboflavin (RB) is a yellow-orange compound that undergoes numerous reactions when exposed to solar radiation. In neutral aqueous solution, riboflavin forms lumichrome (LC) upon photolysis, and in alkaline solution, lumiflavin (LF) is produced.[1−3]

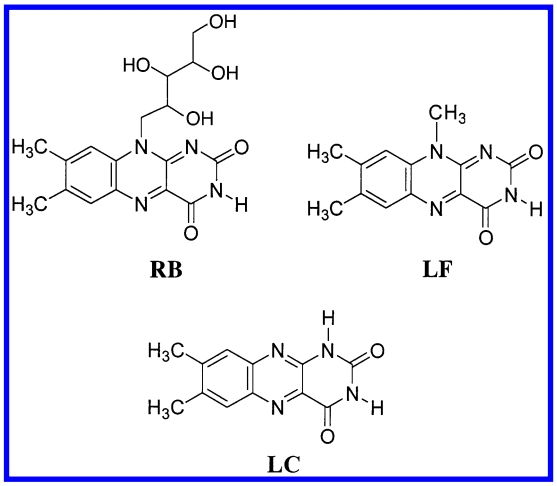

Photolysis of riboflavin and proteins leads to flavin-protein adducts at tryptophan residues. These processes most likely proceed via the triplet state of the flavin as they are quenched by the presence of ascorbate ion (vitamin C), a known triplet quencher.[4−6]

Photolysis of riboflavin and nucleic acids leads to the formation of flavin adducts to AT rich regions of DNA[7] and to the generation of single-strand breaks.[8−11] The single-strand breaks may well be due to the action of superoxide anion or hydrogen peroxide,[7,12−14] which are also formed upon photolysis of riboflavin. Riboflavin and light sensitize the killing of mammalian cells.[15,16] Analysis of the nucleic acids of these cells reveals guanine oxidation and strand breaks.[17,18] Interest in this photochemistry has recently surged due to reports that riboflavin can sensitize the inactivation of viruses in the presence of transfusable blood products with acceptable recovery of plasma protein, platelet, and red cell function.[19]

This has prompted the present study of flavin photochemistry using absorption and fluorescence spectroscopy, laser flash photolysis with UV−vis and infrared spectroscopic detection, and density functional theory (DFT) calculations.

II. Methods

Computational Details. Recent studies have demonstrated that the bond dissociation enthalpies (BDEs) of polycyclic aromatic hydrocarbons (PAHs) can be accurately calculated at the B3LYP level of density functional theory.[20−29] On the basis of the reported agreement between the calculated and experimental PAH BDEs, the B3LYP level was chosen for the calculations of the molecules in this system. B3LYP has the advantage over unrestricted Hartree−Fock methods for aromatic radicals as the latter may suffer from a high degree of spin

* Corresponding authors. Matthew S. Platz (E-mail:platz.1@osu.edu. Fax: 614-292-1685). Christopher M. Hadad (E-mail: hadad.1@osu.edu. Fax: 614-292-1685).

10.1021/jp026051v CCC: $22.00
Published on Web 09/07/2002

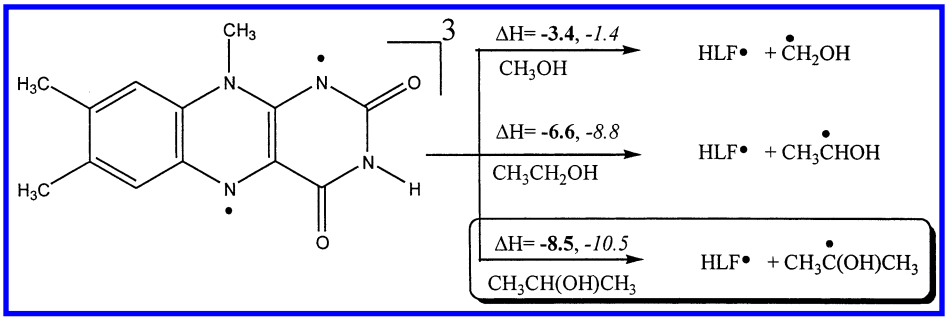

Figure 1. Thermodynamic data (kcal/mol, **B3LYP/6-31G***, *B3LYP/6-31+G**// B3LYP/6-31G**) for the reaction of triplet LF with H-atom donors for the C−H bond adjacent to the OH substituent for simple alcohols forming the most stable hydroflavin radical, HLF•, and the corresponding hydroxyalkyl radical.

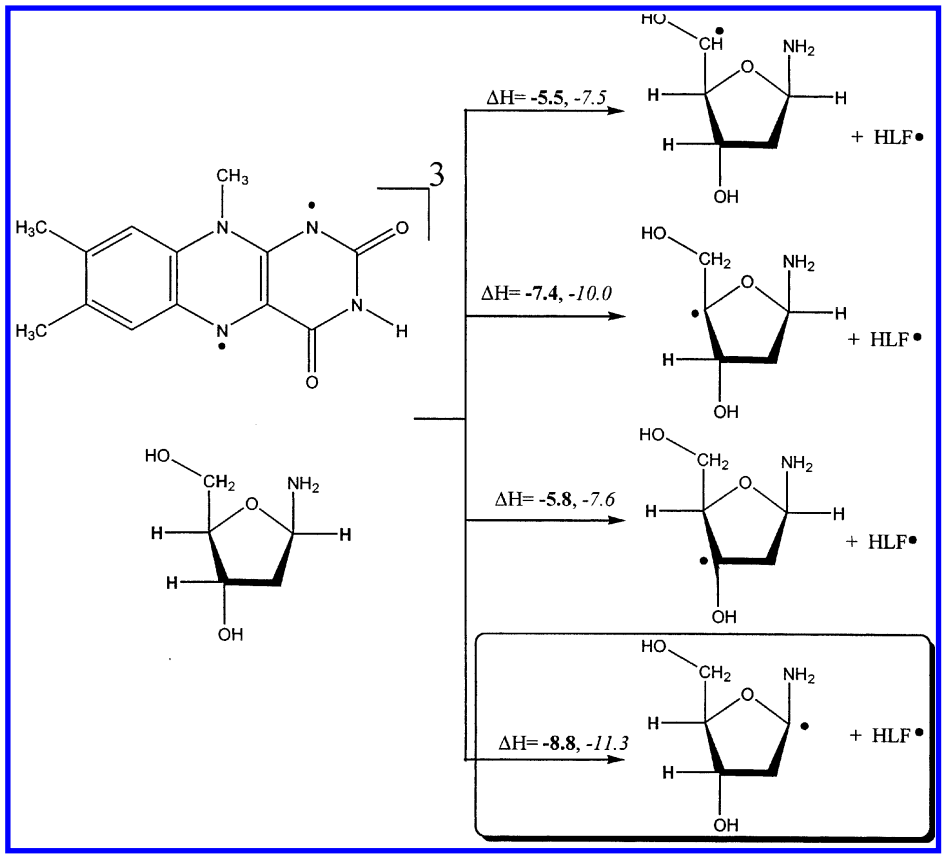

Figure 2. Thermodynamic data (kcal/mol, **B3LYP/6-31G***, *B3LYP/6-31+G**//B3LYP/6-31G**) for the reaction between triplet LF and selected hydrogens on (*R*)-2-amino-(*S*)-4-hydroxy-(*R*)-5-(hydroxymethyl)tetrahydrofuran.

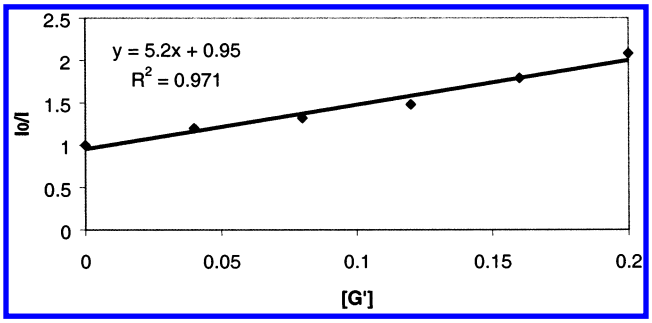

Figure 3. Stern−Volmer fluorescence quenching of RBTA by G′ in CH_2Cl_2.

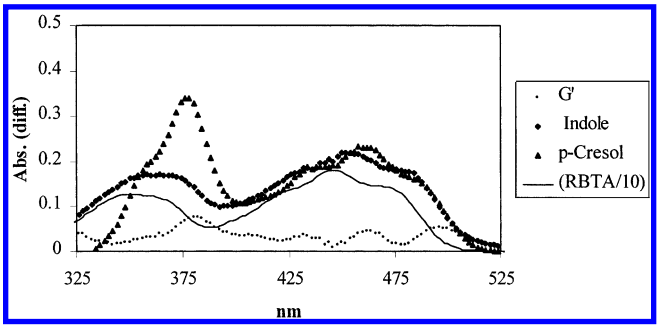

Figure 4. Differential UV−vis absorption spectra of 0.12 mM RBTA in CH_2Cl_2 with 214 mM G′, indole, and *p*-cresol. A scaled (1/10) absolute absorption spectrum of RBTA in CH_2Cl_2 is shown as a reference.

contamination, whereas DFT levels of theory are usually not plagued by this problem.

All calculations were performed using Gaussian 98[30] at the Ohio Supercomputer Center. Geometries were optimized at the B3LYP/6-31G* level of theory, and single-point energies were obtained at the B3LYP/6-31+G** level with the optimized B3LYP/6-31G* geometries.[22,25] Stationary points were verified to be energy minima via vibrational frequency analyses (B3LYP/6-31G*) in which all of the calculated vibrational frequencies were non-imaginary. Zero-point vibrational energy (ZPE) cor-

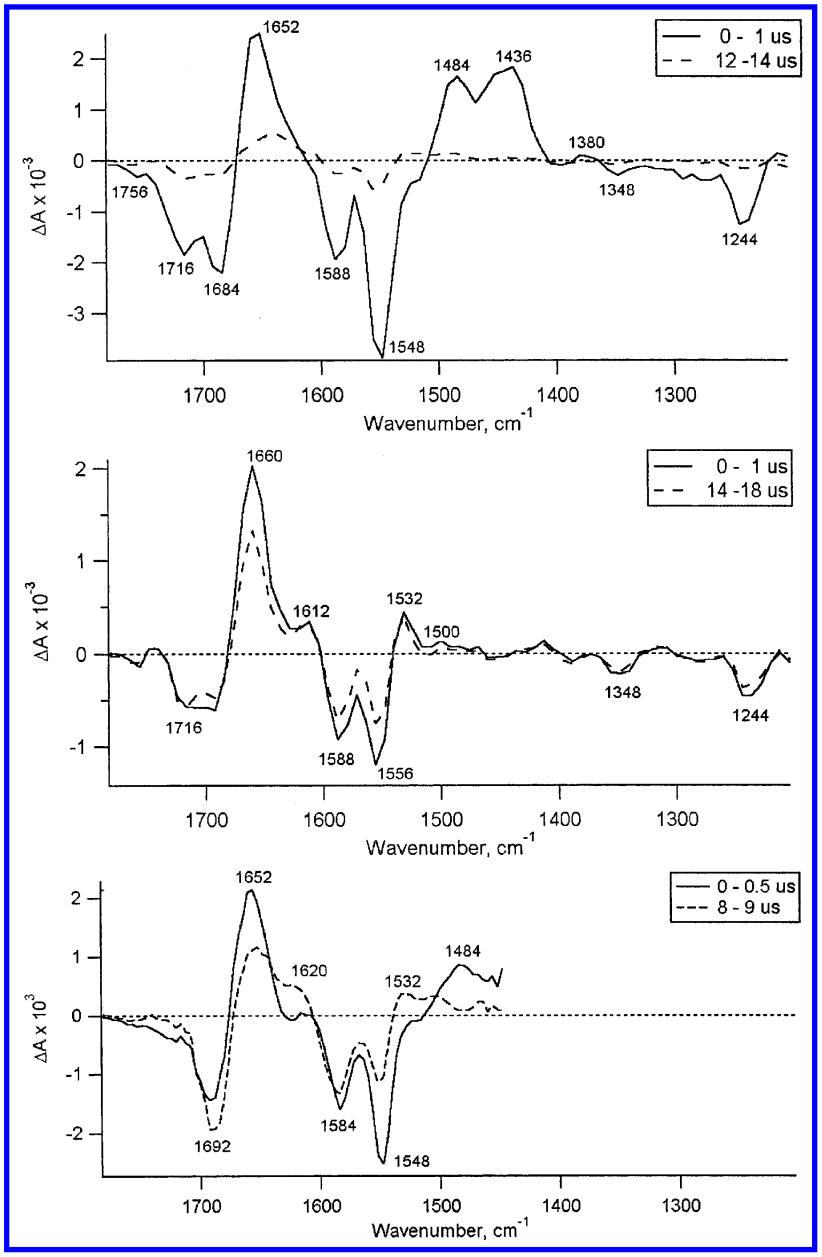

Figure 5. (a) TRIR differential spectra of RBTA in CD_3CN upon 355 nm LFP. (b) TRIR differential spectra of RBTA with indole in CD_3CN upon 355 nm LFP. (c) TRIR differential spectra of 2.5 mM RBTA with 10 mM G′ in deoxygenated methylene chloride upon 355 nm LFP.

rections were also obtained from the vibrational frequency calculations at the B3LYP/6-31G* level, and a scaling factor of 0.9804 was used. Calculated harmonic vibrational frequencies were scaled by 0.9613 in order to compare them to experiment. All reaction enthalpy data represent ΔH at 0 K. Spin contamination for all of the B3LYP optimized structures was low: $0.75 < \langle S^2 \rangle < 0.79$ for the doublet states and $2.0 < \langle S^2 \rangle < 2.1$ for the triplet states. All spin density and charge density data were obtained by a natural population analysis (NPA) at the B3LYP/6-31G* level.[31] (NPA analysis with the 6-31+G** basis set had problems due to the inability to localize the orbitals.) Attempts to calculate the atomic charges and spin densities using Bader's Atoms In Molecules (AIM) methods[32−36] failed due to numerical problems in defining the atomic boundaries.

Experimental Details

TRIR experiments were conducted with a JASCO TRIR-1000 dispersive-type IR spectrometer with 16 cm^{-1} resolution following the method described in the literature.[37−43] Briefly, a reservoir of the deoxygenated sample solution (20 mL 2.5 mM RBTA in CH_2Cl_2, CH_3CN, or CD_3CN with or without the desired quantity of G′ or indole) is continually circulated between two calcium fluoride salt plates with a 0.5 mm path length. The sample was excited by 355 nm laser pulses of a Nd:YAG laser (97 Hz repetition rate, 0.5−0.7 mJ/pulse power), which is crossed with the broadband output of a $MoSi_2$ IR source (JASCO). The intensity change of the IR light induced by photoexcitation is monitored as a function of time by an MCT photovoltaic IR detector (Kolmar Technologies, KMPV11−1-J1), with a 50 ns rise time amplified with a low noise NF Electronic Instruments 5307 differential amplifier, and digitized with a Tektronix TDS784D oscilloscope. The TRIR spectrum is analyzed by the IGOR PRO program (Wavemetrics Inc.) in the form of a difference spectrum:

$$\Delta A_t = -\log(1 + \Delta I_t/I)$$

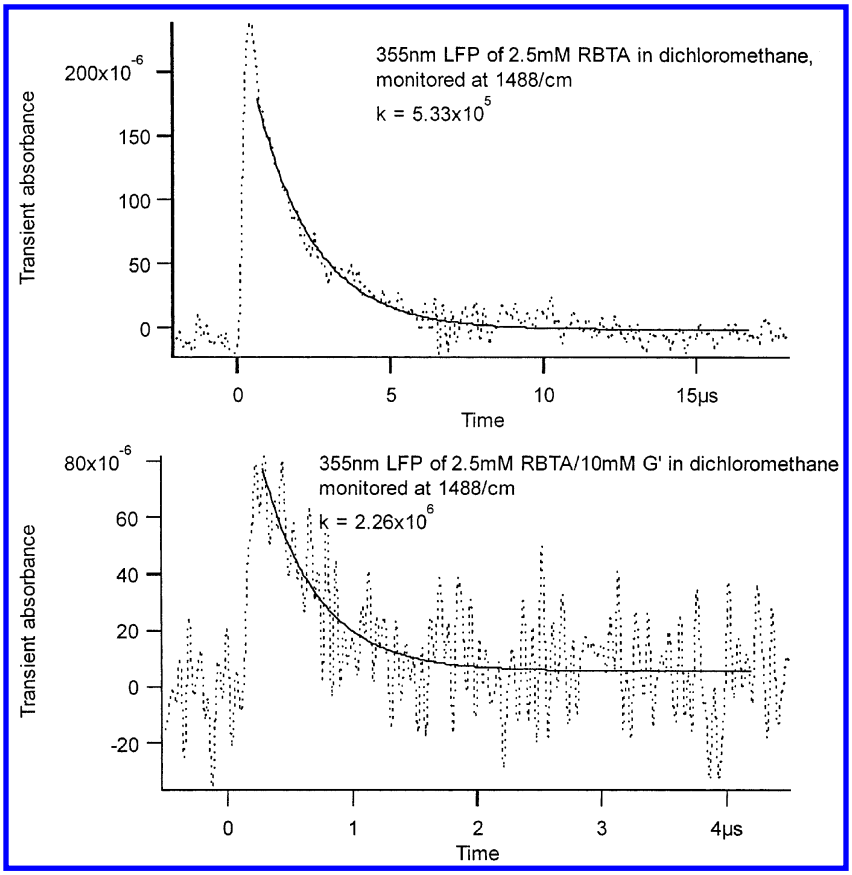

Figure 6. (a) 355 nm LFP of 2.5 mM RBTA in methylene chloride, monitored at 1488 cm^{-1}. (b) 355 nm LFP of 2.5 mM RBTA with 10 mM G′ in methylene chloride, monitored at 1488 cm^{-1}.

where ΔI_t is the intensity change induced by photoreaction at time t, and I is the IR intensity for the sample without photoexcitation. Thus, depletion of reactant and formation of transient intermediates or products lead to negative and positive signals, respectively.

Fluorescence lifetimes were determined using time correlated single photon counting (TCSPC), as described earlier.[44] Fluorescence quenching experiments were carried out using a SPEX Fluorolog 1680 double spectrometer (JY Horiba Inc., Edison, NJ).

The current design of the flash photolysis instrument is based upon the previously described instrument[45] with the following changes. The older version of the instrument was based on a hard-wired computer interface. The upgrade of this basic design is software centered using the LabView graphical programming language, which allows for greater ease in the optimization, integration, and use of the instrument. The new version employs a single ARC SP-308 monochromator/spectrograph, with 1-015-300 grating. This model features dual ports, one with a slit and a photomultiplier for kinetic measurements and the other with a flat field and a Roper ICCD-Max 512T digital ICCD camera for spectroscopic measurements with up to 2 ns temporal resolution. The single monochromator/spectrograph negates the need for separate optimization of kinetic or spectral measurement system alignment, thus facilitating the usage of both types of measurements. The ICCD controller is directly interfaced to the computer using the Roper WinView software and ST-133A controller. Kinetic data acquisition uses a Tektronix TDS 680C 5Gs/s 1GHz oscilloscope directly interfaced via a National PCI-GPIB to a computer running a custom LabView control and acquisition program. Laser, arc lamp, and shutter and other timing and control signals are routed through a National Instruments PCI-6602 DAQ interface. The excitation of the samples was provided by a Spectra Physics LAB-150-10 (∼5 ns) water-cooled laser, which was configured to supply 355 nm radiation. The measurement beam is supplied by a PTI 150 W xenon arc lamp with a LPS 210 power supply, LPS 221 stand alone igniter, A-500 compact arc lamp housing, and MCP-2010 pulser, which allows for controlled pulsing of the arc lamp with pulsed 0.5−2.0 ms in duration and up to 160 amps in amplitude. UV−vis absorption spectra were obtained on a HP 8452 diode array spectrophotometer.

Samples analyzed by LFP were prepared by combining various amounts of a quencher solution of known concentration with a stock solution containing RBTA. The mixture was then diluted to achieve the desired volume and degassed by bubbling argon through the solution for a minimum of 10 min. All kinetic data represent the average of triplicate measurements.

UV−vis absorption shift spectra were performed using a similar sample preparation method.

Binding of G′, indole, and *p*-cresol to RBTA in CH_2Cl_2 was detected as a shift of the UV−vis spectrum of RBTA. A solution of the compound (1.8 mL, 0.238 M) suspected to bind to RBTA was added to a solution of RBTA (0.2 mL, 1.2 mM), and the UV−vis spectrum was recorded. This spectum was compared to the spectrum of RBTA without a binding agent (0.2 mL RBTA solution and 1.8 mL solvent) and the difference spectrum showing the shift in minima and maxima was interpreted as evidence for binding.

Compounds Used in This Study. Compound 2′,3′,4′,5′-tetraacetylriboflavin (riboflavin tetraacetate, RBTA) was synthesized according to the method of McCormick.[46] Silylated guanosine (G′) was synthesized as described by Sheu and

Foote.[47] Adenosine triacetate (ATA) and ribose tetraacetate (RT) were purchased from Aldrich and used as received.

III. Results

In this work, lumiflavin (LF) was used as a model for RB in the calculations because the isoalloxazine (flavin) core, which is responsible for the flavin photochemistry, is assumed to be unperturbed by the removal of the ribityl chain.[48−50] By eliminating the ribityl chain from RB, the calculations become more practical and much faster by removing several hydrogen-bonding interactions, eliminating many possible rotamers, and significantly reducing the overall size of each calculation. Such an approach has been well utilized previously in computational investigations of the flavin core, and most of these studies attempted to understand the mechanism of action of DNA photolyase.[51−57]

In the experimental work, riboflavin tetraacetate (RBTA) will be used instead of RB or LF because the latter two flavins have poor solubility in acetonitrile and methylene chloride, solvents with wide spectral windows in the infrared.

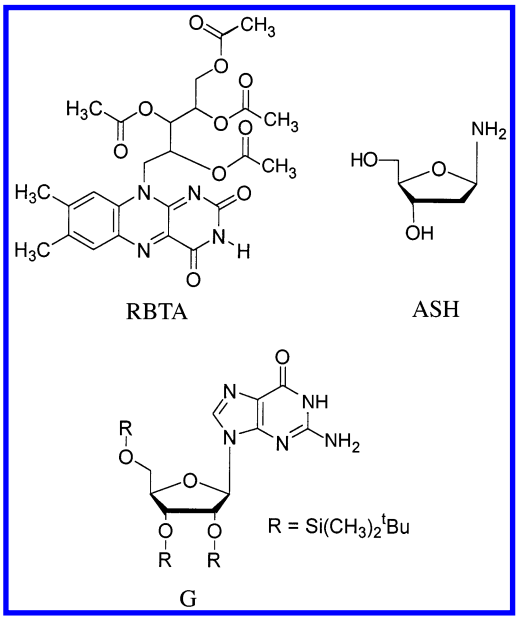

We used a simple amino sugar (ASH)[58] to computationally model the sugar portion of purine nucleosides. In the experimental work, Sheu and Foote's[47] organic soluble guanosine derivative, G′, was utilized along with adenosine triacetate (ATA) and ribose tetraacetate (RT): all of which are soluble in acetonitrile and methylene chloride.

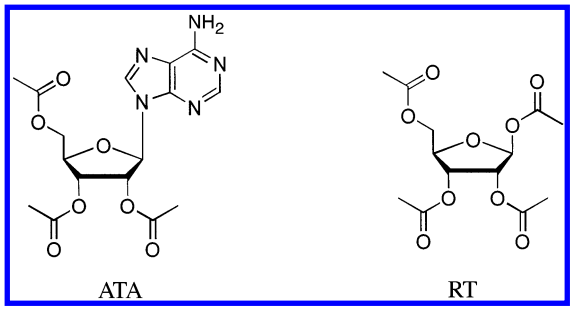

Computational Chemistry. As mentioned in the Introduction, riboflavin and light sensitize single-strand breaks in DNA.[8−11] These may be due to processes involving reactive oxygen species[12,13] or to direct reaction of triplet flavin with the sugar moieties of DNA. Previously, we computed the minimum energy geometry of triplet lumiflavin and the most stable neutral radical (LFH•) formed upon partial reduction of the flavin.[59] This radical is greater than 8 kcal/mol more stable than any other isomeric neutral radical derived from lumiflavin.

SCHEME 1

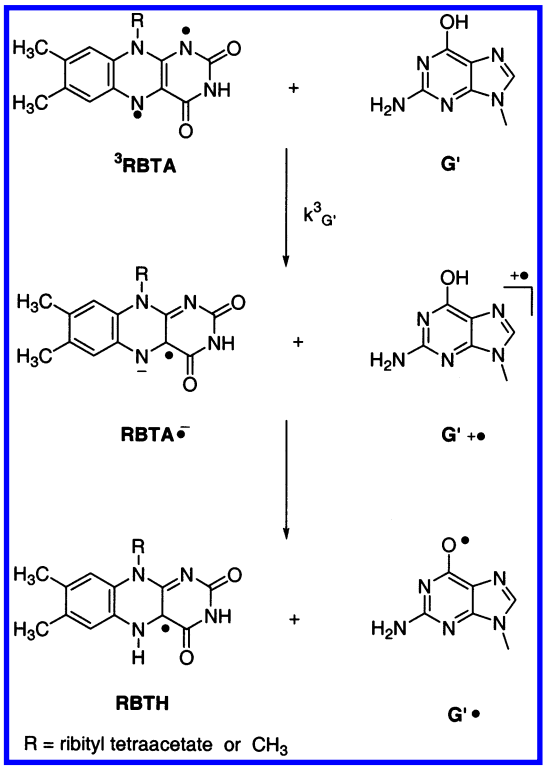

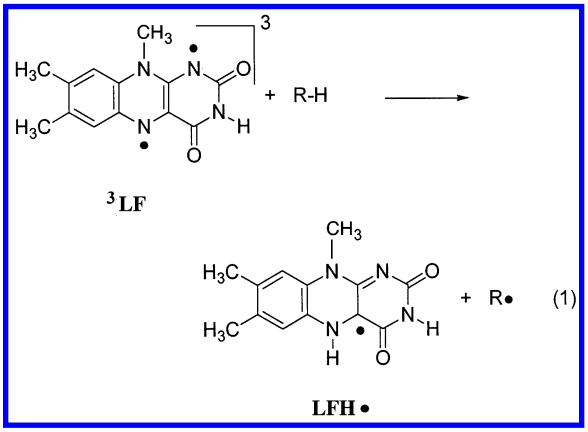

Thus, the heat of reaction (eq 1) with various hydrogen donors (R−H) was readily calculated.

All of the thermodynamic data in Figure 1 indicate that the reaction between triplet LF and the α-hydrogen of a series of simple alcohols to form the hydroxyalkyl radical and LFH• are all exothermic with the most favorable being the reaction with 2-propanol. This thermodynamic trend follows the strength of C−H bonds of the alcohols and the resulting radical stabilities, as expected.[60] As shown in Figure 2, the reactions of triplet LF with cleavage of each of the indicated C−H bonds of the amino sugar ASH are all exothermic in the gas phase, and the most exothermic reaction is at the anomeric ($C_{1'}$) hydrogen of the deoxyribose system.[58] The calculations demonstrate that the reaction of triplet flavin with the sugar backbone of the nucleic acids residues is thermodynamically feasible.

Fluorescence Quenching. Knowles[61] has previously reported that 5′-guanosine monophosphate (GMP) and 5′-adenosine

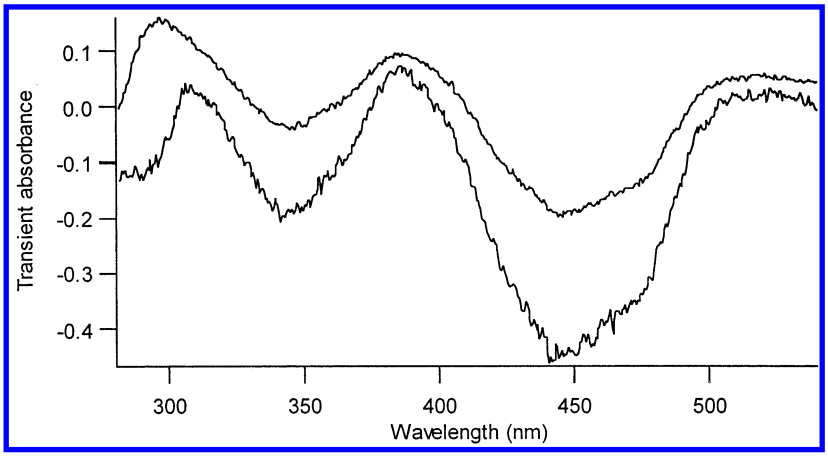

Figure 7. Transient UV−vis absorption spectra of (top) RBTA and (bottom) RBTA + G′ after 355 nm LFP.

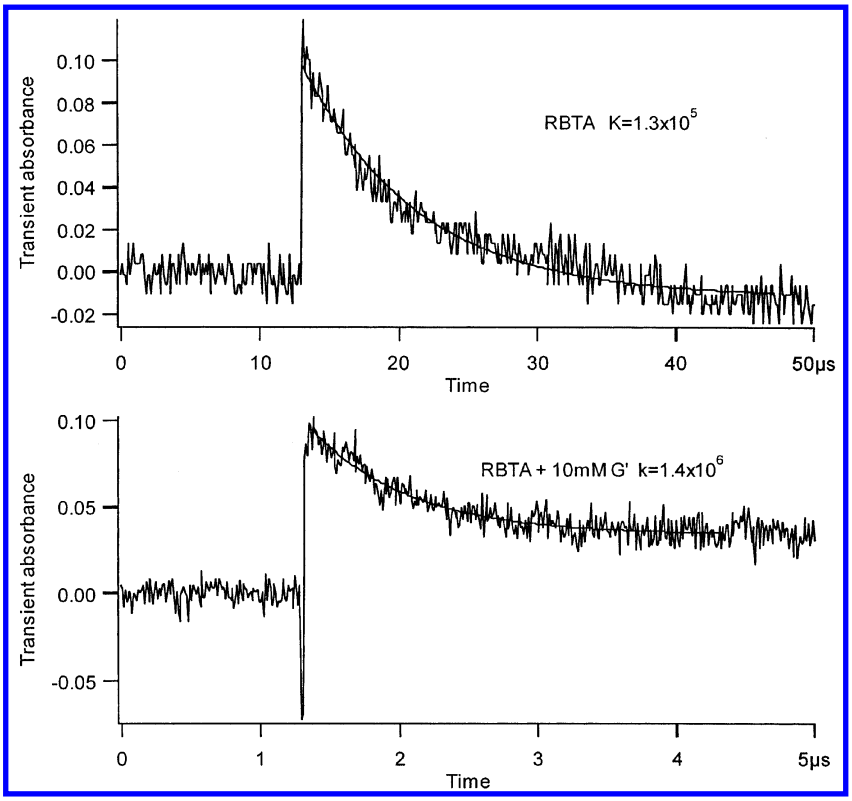

Figure 8. Decay of the signal at 388 nm after 355 nm laser pulse of (top) RBTA and (bottom) RBTA with 10 mM G′ in methylene chloride.

monophosphate (AMP) quench the fluorescence of riboflavin in buffered aqueous solutions. Stern−Volmer analysis of the data led to $k_Q\tau$ values of 65.5 and 82.6 M^{-1}, respectively. Nucleoside concentrations of 0−15 mM led to 50% quenching of the fluorescence. The fluorescence lifetime of riboflavin in water is 5 ns,[62] thus the quenching rate constants with GMP and AMP are 13.1×10^9 and 16.5×10^9 $M^{-1}s^{-1}$, respectively.

We find that G′ quenches the fluorescence of RBTA in methylene chloride (Figure 3). Stern−Volmer analysis of the data yields a $k_Q\tau$ value of 5.2 M^{-1}. Using time correlated single photon counting, we find that the fluorescence lifetimes of RBTA are 6 and 12 ns in CH_2Cl_2 and acetonitrile, respectively. This leads to a value of $k_Q = 0.87 \times 10^9$ M^{-1} s^{-1}, which is ≈15-fold smaller than the rate constant for quenching of excited singlet riboflavin with GMP in aqueous buffer reported by Knowles.[61]

Dardare has found that riboflavin associates with GMP in aqueous buffer.[63] This association is manifest as a GMP dependent shift in the absorption spectrum of riboflavin. As shown in Figure 4, indole and *p*-cresol (200 mM) will induce similar shifts in the spectrum of RBTA in methylene chloride, but a comparable concentration of G′ does not. It seems clear that RBTA and indole (and *p*-cresol) associate in methylene chloride, but there is no evidence of association of RBTA and G′ in this solvent. Thus, the greater fluorescence quenching rate constants observed by Knowles likely reflects the preassociation of riboflavin and GMP in aqueous buffer solution.

Time-Resolved Infrared Spectroscopy. We have previously reported that laser flash photolysis (LFP) of RBTA at 355 nm in deoxygenated CD_3CN produced the transient spectrum of $^3RBTA^*$ with $\tau = 2$ μs.[59] $^3RBTA^*$ has intense C═O vibrations at 1652 cm^{-1} and C═N vibrations at 1484 and 1436 cm^{-1} (Figure 5a), in satisfactory agreement with density functional theory calculations.[59]

Upon LFP of RBTA in the presence of an electron donor such as sodium iodide, the transient spectrum of the RBTA radical anion ($RBTA^{\cdot -}$) was detected ($\nu_{C=O} = 1636$ cm^{-1}, $\tau = 20$ μs). The most important resonance structure of $RBTA^{\cdot -}$

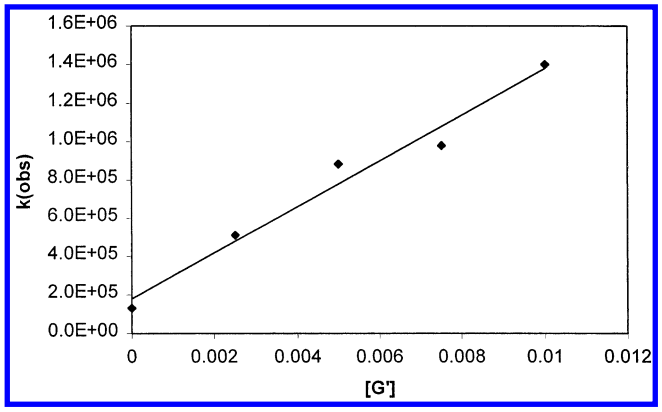

Figure 9. Plot of k_{obs} vs [G′] (k_{obs} is the decay constant of 388 nm signal in deoxygenated methylene chloride of RBTA + G′).

(as deduced by DFT calculations of LF•$^-$) is depicted in Scheme 1. Previously, we have reported that LFP of RBTA in CD_3CN containing 20 mM indole produces the TRIR spectrum of neutral radical RBTH, produced by protonation of the flavin radical anion.[59] In that study, we used DFT calculations to evaluate the energies of every neutral radical obtained by protonation of each oxygen and nitrogen of the lumiflavin radical anion. The thermodynamically most stable radical (by 8 kcal/mol) corresponds to protonation of N_5, as shown for RBTH (Scheme 1). Furthermore, this is the only low energy, neutral flavin radical predicted with a carbonyl vibration close (1650 cm^{-1}) to the experimental value of 1660 cm^{-1} (Figure 5b). The indoyl radical was not detected.[59]

LFP (355 nm) of 2.5 mM RBTA in deoxygenated CH_2Cl_2 containing 10 mM G′ produces the transient IR spectrum of the RBTH radical shown in Figure 5c. This concentration of G′ is not sufficient to quench the excited singlet state of RBTA to a significant extent based on the fluorescence quenching information. Thus, RBTH is undoubtedly formed from ^{3}RBTA* by the sequential electron transfer−proton transfer mechanism depicted in Scheme 1.

As predicted by Scheme 1, ^{3}RBTA* decays exponentially (Figure 6) and the observed rate constant of disappearance of G′, measured at 1488 cm^{-1}, increases in the presence of G′. From Figure 6, one can very crudely estimate that the rate constant for electron transfer ($k^3_{G'}$, Scheme 1) is on the order of 10^8 M^{-1} s^{-1}. Because G′ quenches ^{1}RBTA*, the yield of ^{3}RBTA* is low and the signal-to-noise of the decay trace becomes less favorable in the presence of G′.

In related experiments, we found that adenosine triacetate (ATA) also accelerates the decay of triplet RBTA ($k^3_{ATA} \approx 10^6$ M^{-1} s^{-1}) in acetonitrile. The lower reactivity of ATA relative to G′ reflects the relative ease of oxidation of these reagents.[64,65] Ribose tetraacetate (RT) does not accelerate the decay of ^{3}RBTA*, even at concentrations as large as 100 mM. Thus, even though hydrogen-atom abstraction reactions of ^{3}RBTA with sugars are predicted to be exothermic, these reactions are relatively unimportant mechanisms of quenching ^{3}RBTA* with purine nucleosides in solution.

The similarity of the TRIR spectrum observed upon the LFP of RBTA in the presence of G′, indole, and *p*-cresol leads us to assign the main features of the transient spectrum to the flavin nucleus. The calculated vibrational spectrum of the neutral G′ radical is given in the Supporting Information and does not conform to the experimental spectrum. This is further evidence that we are detecting the TRIR spectrum of the flavin radical.

Laser Flash Photolysis with UV−Vis Detection. Flavins have been extensively studied by LFP methods with UV−vis detection in aqueous and organic solvents.[1] LFP (355 nm) of RBTA in methylene chloride was performed. As expected, ^{3}RBTA* has transient absorption maxima at 310 and 390 nm as well as a broad absorbance above 500 nm (Figure 7).[1,2,66,67] The presence of G′ accelerates the disappearance of the transient absorption (Figures 7 and 8), although the transient absorption no longer decays to baseline. A plot of the observed rate constant of disappearance of ^{3}RBTA* versus [G′] is linear (Figure 9). The slope of this plot, $k^3_{G'}$, is 1.0×10^8 M^{-1}s^{-1} and is consistent with the TRIR studies. The transient spectrum observed after ^{3}RBTA* has decayed is assigned to the longer-lived neutral flavin radical RBTH. Triplet RBTA and the radical RBTH have similar spectra; hence, ^{3}RBTA* does not decay to baseline in the presence of G′.

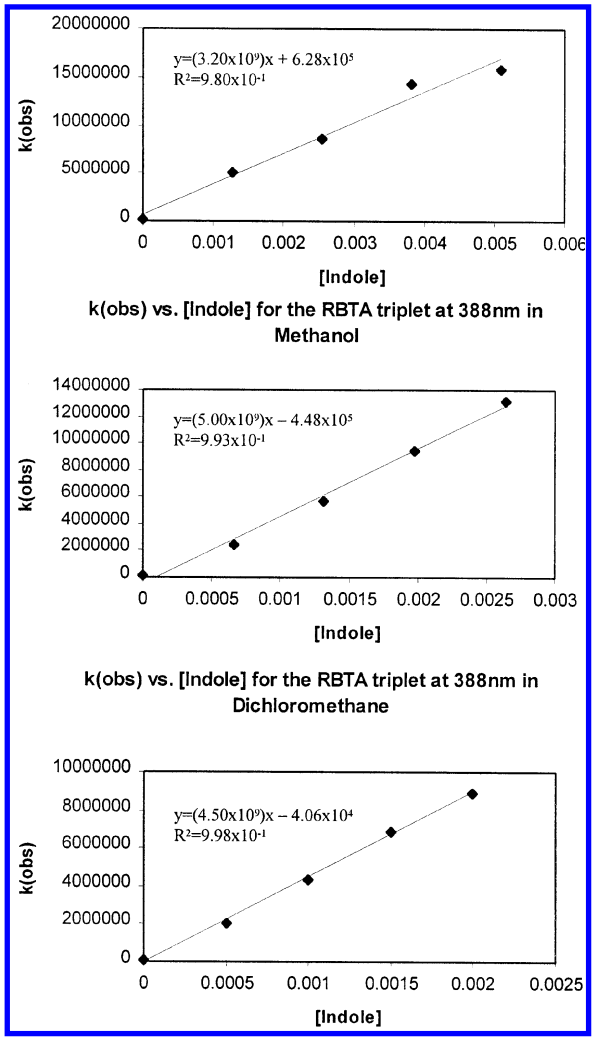

Figure 10. k_{obs} vs [indole] of RBTA at 388 nm after 355 nm LFP in selected solvents.

The rate of decay of triplet RBTA (LFP, 355 nm) was monitored at 388 nm as a function of indole concentration in methanol, acetonitrile, and methylene chloride. The data (Figure 10) show that $k^3_{indole} = 3.2 \times 10^9$ M^{-1} s^{-1} in acetonitrile, 5.0×10^9 M^{-1} s^{-1} in methanol, and 4.5×10^9 M^{-1} s^{-1} in methylene chloride. All plots contained five data points, each point was an average of three separate decay rates from separate experiments, and all had an R^2 value of 0.980 or better (Figure 10). Triplet RBTA, therefore, reacts much more rapidly with indole than with G′ in dichloromethane. This may reflect an intrinsically higher reactivity of indole, relative to AMP and GMP. It also reflects the fact that indole associates with RBTA, but there

is no evidence that G′ undergoes complexation at the concentrations employed in this study.

RBTA in methylene chloride was also pulsed with 355 nm light in the presence of 300 mM G′. Under these conditions, greater than 70% of the fluorescence of singlet RBTA has been quenched. The transient spectrum (Supporting Information) is that of the neutral hydroflavin radical, RBTH. The intensity of the RBTH spectrum obtained in the presence of 300 mM G′ is only ≈20% that obtained in the presence of 10 mM G′. It is possible that the yield of RBTH from ^{1}RBTA* is only 20% that of radical formation from ^{3}RBTA. It seems more likely that G′ quenching of ^{1}RBTA* does not produce RBTH on the ns time scale and that the small yield of radical observed is entirely due to the low yield of ^{3}RBTA in the presence of 300mM G′.

Conclusions

Hydrogen-atom transfer reactions of triplet lumiflavin with (*R*)-2-amino-(*S*)-4-hydroxy-(*R*)-5-(hydroxymethyl)-tetrahydrofuran, as a model for the sugar ring of DNA, were predicted to be exothermic by density functional theory calculations at the B3LYP/6-31+G**//B3LYP/6-31G* level of theory. Nevertheless, the reaction of triplet riboflavin tetraacetate (^{3}RBTA*) with ribose tetraacetate was too slow to measure by time-resolved infrared (TRIR) spectroscopy. Absolute rate constants of ^{3}RBTA* with indole and with a silylated guanosine derivative (G′) were determined to be 4.5×10^9 and 1.0×10^8 M^{-1} s^{-1}, respectively, in methylene chloride at ambient temperature. TRIR spectroscopy demonstrated that ^{3}RBTA* reacts with G′ to form a hydroflavin radical RBTH by an electron transfer−proton transfer mechanism. LFP−UV results are consistent with the TRIR data. Both indole and G′ quench the fluorescence of ^{1}RBTA* in methylene chloride ($\tau = 12$ ns). In the case of G′, singlet chemistry leads to only modest yields of the RBTH radical.

Acknowledgment. The authors are indebted to Mr. Frank DeLucia Jr., Dr. James S. Poole, and Professor Terry Gustafson for determining the fluorescence lifetime of RBTA in methylene chloride and acetonitrile. One of us (M.L.T.) gratefully acknowledges a Presidential Fellowship of The Ohio State University. Computational support from the Ohio Supercomputer Center is gratefully acknowledged.

Supporting Information Available: Figure S1: Ground state FT-IR of G′. Figure S2: Calculated vibrational region from 1400−1800 cm^{-1} of 5H-LF•, phenoxy, and G′ radicals. This material is available free of charge via the Internet at http://pubs.acs.org.

References and Notes

(1) Heelis, P. F. *Chem. Soc. Rev.* **1982**, *11*, 15−39.
(2) Heelis, P. F. *Chem. Biochem. Flavoenzymes* **1991**, *1*, 171−193.
(3) Song, P.-S.; Metzler, D. E. *Photochem. Photobiol.* **1967**, *6*, 691−709.
(4) Tapia, G.; Silva, E. *Radiat. Environ. Biophys.* **1991**, *30*, 131−138.
(5) Silva, E.; Salim-Hanna, M.; Edwards, A. M.; Becker, M. I.; De Ioannes, A. E.; Friedman, N. *A Light-Induced Tryptophan-Riboflavin Binding: Biological Implications*; Plenum: New York, 1991.
(6) Salim-Hanna, M.; Edwards, A. M.; Silva, E. *Int. J. Vitam. Nutr. Res.* **1987**, *57*, 155−159.
(7) Ennever, J. F.; Carr, H. S.; Speck, W. T. *Pediat. Res.* **1983**, *17*, 192−194.
(8) Joshi, P. C. *Indian J. Biochem. Biophys.* **1989**, *26*, 186−189.
(9) Speck, W. T.; Rosenkranz, S.; Rosenkranz, H. S. *Biochim. Biophys. Acta* **1976**, *435*, 39−44.
(10) Korycka-Dahl, M.; Richardson, T. *Biochim. Biophys. Acta* **1980**, *610*, 229−230.
(11) Kochevar, I. E.; Dunn, D. A. In *Bioorganic Photochemistry*; Morrison, H., Ed.; Wiley: New York, 1990; Vol. 1, pp 273−316.
(12) Joshi, P. C. *Toxicol. Lett.* **1985**, *26*, 211−217.
(13) Korycka-Dahl, M.; Richardson, T. *J. Food Prot.* **1980**, *43*, 19−20.
(14) Kasai, H.; Crain, P. F.; Kuchina, Y.; Nishimura, S.; Outsuyama, A.; Tanoka, H. *Carcinogenesis* **1986**, *7*, 1847−1851.
(15) Edwards, A. M.; Silva, E. J., B.; Becker, M. I.; De Ioannes, A. E. *J. Photochem. Photobiol. B* **1994**, *24*, 179−186.
(16) Sato, K.; Taguchi, H.; Maeda, T.; Minami, H.; Asada, Y.; Watanabe, Y.; Yoshikawa, K. *J. Invest. Dermatol.* **1995**, *105*, 608−612.
(17) Yamamoto, F.; Nishimura, S.; Kasai, H. *Biochem. Biophys. Res. Commun.* **1992**, *187*, 809−813.
(18) Hoffmann, M. E.; Meneghini, R. *Photochem. Photobiol.* **1979**, *29*, 299−303.
(19) Goodrich, R. P. In *Cambridge Healthtech Institute's Sixth Annual Blood Product Safety Conference*, 2000.
(20) Barckholtz, C.; Barckholtz, T. A.; Hadad, C. M. *J. Am. Chem. Soc.* **1999**, *121*, 491−500.
(21) Becke, A. D. *J. Chem. Phys.* **1988**, *88*, 2547.
(22) Becke, A. D. *J. Chem. Phys.* **1993**, *98*, 5648−5652.
(23) Johnson, B. G.; Gill, P. M. W.; Pople, J. A. *J. Chem. Phys.* **1993**, *98*, 5612−5626.
(24) Stephens, P. J.; Devlin, F. J.; Chabalowski, C. F.; Frisch, M. J. *J. Phys. Chem.* **1994**, *98*, 11623−11627.
(25) Lee, C.; Yang, W.; Parr, R. G. *Phys. Rev. B* **1988**, *37*, 785−789.
(26) Bauschlicher, C. W., Jr.; Langhoff, S. R. *Mol. Phys.* **1999**, *96*, 471−476.
(27) Cioslowski, J.; Liu, G.; Moncrieff, D. *J. Org. Chem.* **1996**, *61*, 4111−4114.
(28) Cioslowski, J.; Liu, G.; Martinov, M.; Piskorz, P.; Moncrieff, D. *J. Am. Chem. Soc.* **1996**, *118*, 561−5264.
(29) Wiberg, K. B.; Cheeseman, J. R.; Ochterski, J.; Frisch, M. J. *J. Am. Chem. Soc.* **1995**, *117*, 6535−6543.
(30) Frisch, M. J.; Trucks, G. W.; Schlegel, H. B.; Scuseria, G. E.; Robb, M. A.; Cheeseman, J. R.; Zakrzewski, V. G.; J. A. Montgomery, J.; Stratmann, R. E.; J. C. Burant, S. D.; Millam, J. M.; Daniels, A. D.; Kudin, K. N.; Strain, M. C.; O. Farkas, J. T.; V. Barone, M. C.; Cammi, R.; Mennucci, B.; Pomelli, C.; Adamo, C.; Clifford, S.; Ochterski, J.; Petersson, G. A.; Ayala, P. Y.; Cui, Q.; Morokuma, K.; Malick, D. K.; Rabuck, A. D.; Raghavachari, K.; Foresman, J. B.; Cioslowski, J.; Ortiz, J. V.; Baboul, A. G.; Stefanov, B. B.; Liu, G.; Liashenko, A.; Piskorz, P.; Komaromi, I.; Gomperts, R.; Martin, R. L.; Fox, D. J.; Keith, T.; Al-Laham, M. A.; Peng, C. Y.; Nanayakkara, A.; Challacombe, M.; Gill, P. M. W.; Johnson, B.; Chen, W.; Wong, M. W.; Andres, J. L.; Gonzalez, C.; Head-Gordon, M.; Replogle, E. S.; Pople, J. A. *SGI64-G98*, revision A.9; Gaussian, Inc.: Pittsburgh, PA, 1998.
(31) Reed, A. E.; Weinhold, F.; Curtiss, L. A. *Chem. Rev.* **1988**, *88*, 899.
(32) Cioslowski, J.; Piskorz, P. *Chem. Phys. Lett.* **1996**, *255*, 315−319.
(33) Bader, R. F. W. *Atoms in Molecules−A Quantum Theory*; Clarendon Press: Oxford, 1990.
(34) Bader, R. F. W. *Acc. Chem. Res.* **1985**, *18*, 9−15.
(35) Wiberg, K. B.; Rablen, P. R. *J. Comput. Chem.* **1993**, *14*, 1504−1518.
(36) Bader, R. F. W. *Chem. Rev.* **1991**, *91*, 893−928.
(37) Yuzawa, T.; Kato, C.; George, M. W.; Hamaguchi, H. *Appl. Spectrosc.* **1994**, *48*, 684−690.
(38) Toscano, J. P. *Adv. Photochem.* **2001**, *26*, 41.
(39) Ford, P. C.; Bridgewater, J. S.; Lee, B. *Photochem. Photobiol.* **1997**, *65*, 57.
(40) George, M. W.; Poliakoff, M.; Turner, J. J. *Analyst* **1994**, *119*, 551−560.
(41) George, M. W.; Turner, J. J. *Coord. Chem. Rev.* **1998**, *177*, 201−217.
(42) Schoonover, J. R.; Strouse, G. F. *Chem. Rev.* **1998**, *98*, 1335−1355.
(43) Iwata, K.; Hamaguchi, H. *Appl. Spectrosc.* **1990**, *44*, 1431.
(44) Buterbaugh, J. S.; Toscano, J. P.; Weaver, W. L.; Gord, J. R.; Hadad, C. M.; Gustafson, T. L.; Platz, M. S. *J. Am. Chem. Soc.* **1997**, *119*, 3580−3591.
(45) Gritsan, N. P.; Zhai, H. B.; Yuzawa, T.; Karweik, D.; Brooke, J.; Platz, M. S. *J. Phys. Chem. A* **1997**, *101*, 2833.
(46) McCormick, D. B. *Heterocycl. Chem.* **1970**, *7*, 447.
(47) Sheu, C.; Foote, C. S. *J. Am. Chem. Soc.* **1995**, *117*, 6439.
(48) Neither RBTA nor LF will interact with a ring nitrogen by hydrogen bonding. There may be intramolecular hydrogen bonding of a ribityl hydroxyl group with a ring nitrogen under some conditions, but no evidence of such intramolecular hydrogen bonding is seen in the X-ray crystal structure of riboflavin. (See refs 49 and 50.)
(49) Fujii, S.; Kawasaki, K.; Sato, A.; Fujiwara, T.; Tomita, K.-I. *Arch. Biochem. Biophys.* **1977**, *181*, 363.
(50) Voet, D.; Rich, A. *Proc. Natl. Acad. Sci. U.S.A.* **1971**, *68*, 1151.

(51) Lee, E.; Medvedev, E. S.; Stuchebrukhov, A. A. *J. Phys. Chem. B* **2000**, *104*, 6894−6902.
(52) Weber, S.; Mobius, K.; Richter, G.; Kay, C. W. M. *J. Am. Chem. Soc.* **2001**, *123*, 3790−3798.
(53) Meyer, M.; Hartwig, H.; Schomburg, D. *J. Mol. Struct. (THEOCHEM)* **1996**, *364*, 139−149.
(54) Rotello, V. M. *Heteroatom Chem.* **1998**, *9*, 605−606.
(55) Meyer, M. *J. Mol. Struct. (THEOCHEM)* **1997**, *417*, 163−168.
(56) Platenkamp, R. J.; Palmer, M. H.; Visser, A. W. G. *J. Mol. Struct.* **1980**, *67*, 45−64.
(57) Zuber, G.; Lui, J.; Hadad, C. M. Unpublished results (Ohio State University).
(58) Zheng, Y. J.; Ornstein, R. L. *J. Am. Chem. Soc.* **1996**, *118*, 9402−9408.
(59) Martin, C. B.; Tsao, M.-L.; Hadad, C. M.; Platz, M. S. *J. Am. Chem. Soc.* **2002**, *124*, 7226−7234.
(60) McMillen, D. F.; Golden, D. M. *Annu. Rev. Phys. Chem.* **1982**, *33*, 493.
(61) Knowles, A. *Photochem. Photobiol.* **1971**, *13*, 225.
(62) Wahl, P.; Auchet, J. C.; Visser, A. W. J. G.; Muller, F. *FEBS Lett.* **1974**, *44*, 23.
(63) Dardare, N.; Platz, M. S. *Photochem. Photobiol.* **2002**, *75*, 561.
(64) Steenken, S.; Jovanovic, S. V. *J. Am. Chem. Soc.* **1997**, *119*, 617.
(65) Steenken, S. *Chem. Rev.* **1989**, *89*, 503−520.
(66) Heelis, P. F.; Parsons, B. J.; Phillips, G. O. *Biochim. Biophys. Acta* **1979**, *587*, 455.
(67) Knowles, A.; Roe, E. M. F. *Photochem. Photobiol.* **1968**, *7*, 421.